ISSN 0021-3640, JETP Letters, 2020, Vol. 112, No. 6, pp. 341–345. © Pleiades Publishing, Inc., 2020.
Russian Text © The Author(s), 2020, published in Pis'ma v Zhurnal Eksperimental'noi i Teoreticheskoi Fiziki, 2020, Vol. 112, No. 6, pp. 361–366.

OPTICS AND LASER PHYSICS

Virtual Image within a Transparent Dielectric Sphere

A. R. Bekirov[a], *, B. S. Luk'yanchuk[a], and A. A. Fedyanin[a]

[a] *Faculty of Physics, Moscow State University, Moscow, 119991 Russia*

**e-mail: arlen.bekirov@mail.ru*

Received August 22, 2020; revised August 27, 2020; accepted August 28, 2020

From the standpoint of the wave theory, we discuss the problem of an optical image formation created by a virtually converging electromagnetic wave from a light source. We solved a diffraction problem of a point source in a dielectric sphere. Formulas are obtained describing the virtual image of a point source in dielectric sphere, in the parameter range where the approximation of geometric optics is not valid. For slits in an opaque screen, the virtual image in the dielectric sphere allows the resolution of slits spaced from each other at distances much smaller than the diffraction limit $\lambda/2$. This explains the previously obtained experimental results [Z. B. Wang, W. Guo, L. Li, B. Luk'yanchuk, A. Khan, Z. Liu, Z. Chen, and M. H. Hong, Nat. Commun. **2**, 218 (2011)] on the super resolution effect with virtual image.

DOI: 10.1134/S0021364020180058

In 1609, Galileo used a refracting telescope consisting of a convex objective lens and a concave eyepiece, forming a virtual, enlarged image of the object. In 1611, Kepler formulated the rules of an optical image formation within the lens on the basis of the light refraction law and light straightforward propagation. Applying these rules to the transparent sphere, it is easy to find the virtual image plane position $z_{vi} = nR/(2-n)$ and the corresponding magnification factor $M = n/(2-n)$. Here, n is a refractive index and R is the radius of the sphere. Seneca wrote about the magnifying effect of such spheres about two thousand years ago [1]. The formulas written above have a limited range of applicability: they are not applicable as $n \to 2$, since in this case $M \to \infty$, as well as for the sphere size of the order of several wavelengths of light λ; geometric optics formulas work when $R \gg \lambda$.

Modern technologies make it possible to manufacture spherical particles with sizes from tens of nanometers to tens of micrometers, which is widely used in nanophotonics research [2]. Already the first experiments [3] showed that an increase in resolution of a virtual image using small spherical micro lenses with a size of the order of several micrometers allows one to overcome the diffraction limit and viewed the structures of the size of tens of nanometers with the help of usual microscope. It has been studied in numerous works cited in [4], and received good experimental confirmation. However, a theoretical description of this phenomenon requires a description of the virtual image within the wave theory framework. We are not aware of any works devoted to the study of this problem.

The Mie theory [5, 6] considers the exact solution of Maxwell's equations for the case of scattering of a plane electromagnetic wave by a spherical particle. This theory can be generalized by considering the scattering of a diverging spherical wave from the point source inside a sphere or at some distance from it [7, 8]. In these works, another model of a point source was adopted, which does not consider the important contribution of the longitudinal modes. Moreover, in [7, 8] the construction of a virtual image was not considered as well it must be constructed as a virtual convergent electromagnetic wave from the scattered light.

Let $\mathbf{E}_s$ be the field of some source, and Γ be the surface of the aperture of the optical device. Let us introduce field $\mathbf{E}_i$ using the Kirchhoff–Helmholtz theorem [5]

$$\mathbf{E}_i = \frac{1}{4\pi}\iint_\Gamma (G(\mathbf{n},\nabla)\mathbf{E}_s^* - \mathbf{E}_s^*(\mathbf{n},\nabla)G)k^2 dS, \qquad (1)$$

where $G = \exp[ik|\mathbf{r}-\mathbf{r}_0|]/k|\mathbf{r}-\mathbf{r}_0|$ is the Green's function of the wave equation, the operator is $\nabla = \frac{1}{k}\left(\frac{\partial}{\partial x}, \frac{\partial}{\partial y}, \frac{\partial}{\partial z}\right)$ and $k = 2\pi/\lambda$ is the wave number. As known [5, 6], integral (1) does not depend on the shape of the surface, and (in the case of an infinite or closed surface), also on the distance from the surface to the source. For example, let the source be radiation emanating from the slit of an opaque screen. The field of such a source can be defined as

$$\mathbf{E}_s = \frac{(-2)}{4\pi}\iint_\Sigma (\mathbf{E}^0(\mathbf{n},\nabla)G)k^2 dS. \qquad (2)$$

Here, $\mathbf{E}^0$ is the field in the plane of the hole. In the case of Kirchhoff boundary conditions [5], we can accept the simplest model: $\mathbf{E}^0 = \text{const}$. The $\mathbf{E}_s$ field represents a superposition of point sources of the form of $(\mathbf{n},\nabla)G$. Let Γ be an infinite plane, being, in fact, the aperture of the optical device, if the field $\mathbf{E}_s = G\mathbf{e}_x$, then in the plane of the source parallel to the plane Γ, the image field $\mathbf{E}_i$ can be analytically represented as

$$\mathbf{E}_i = -i\frac{\sin(k|\mathbf{r}-\mathbf{r}_0|)}{k|\mathbf{r}-\mathbf{r}_0|}\mathbf{e}_x. \quad (3)$$

This image field from the point delta source is determined by the function $\sin(k|\mathbf{r}-\mathbf{r}_0|)$, which has a half-width $\lambda/2$. Hence, the Rayleigh criterion follows: resolution limit of two incoherent point sources is equal to $\lambda/2$. This criterion applies to lateral resolution, longitudinal resolution in this case, significantly less than $\lambda/2$. If Γ presents a closed surface surrounding the sources, then the diffraction limit $\lambda/2$ preserves in any direction. In the case of $\mathbf{E}_s = (\mathbf{n},\nabla)G$ source, an analytical solution similar to (3) cannot be found, but Eq. (1) can be numerically integrated. Numerical integration leads to results, qualitatively similar to (3), but the first zero of distribution $\mathbf{E}_i$ is situated at the point $|x| = 1.22\lambda/2$, see Fig. 1.

Now, we can complicate the task by setting a dielectric sphere of radius R between the point source and the optical aperture. In this case, one can still use Eq. (1), in which, however, one should substitute the field $\mathbf{E}_s$, caused by diffraction of radiation on the sphere. Without limiting the generality, we represent the source term in the form:

$$\mathbf{E}^i = pkr_0\frac{\partial G(\mathbf{r},\mathbf{r}_0)}{k\partial z_0}\mathbf{e}_x. \quad (4)$$

To pass to the original normalization, it is sufficient to put $p = 1/kr_0$ for simplicity we consider the source situated on the z axis, i.e., $\mathbf{r}_0 = (0,0,-r_0)$. The fields related to the space outside the sphere will be denoted by index 1, and the fields inside the sphere by index 2. Both fields satisfy wave equations with the refractive indices n_1 and n_2, and the permeabilities μ_1 and μ_2. To find these fields we use the standard decomposition in the eigenfunctions $\mathbf{M}$, $\mathbf{N}$, and $\mathbf{L}$ in the spherical coordinate system $\{r,\theta,\varphi\}$ in the same way as it is done within the Mie theory [9]:

$$\mathbf{E}^{(1)} = \mathbf{E}^i + \sum_{\ell=1}^{\infty}(a_\ell\mathbf{N}_\ell + b_\ell\mathbf{M}_\ell + f_\ell\mathbf{L}_\ell), \quad r > R, \quad (5)$$

$$\mathbf{E}^{(2)} = \sum_{\ell=1}^{\infty}(d_\ell\mathbf{N}_\ell + c_\ell\mathbf{M}_\ell + t_\ell\mathbf{L}_\ell), \quad r < R. \quad (6)$$

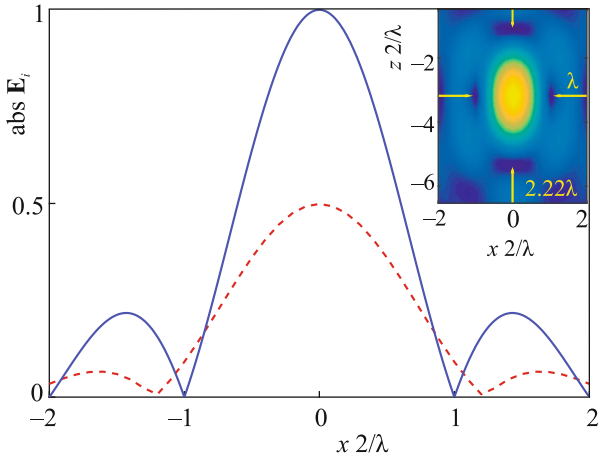

Fig. 1. (Color online) Comparison of the abs$\mathbf{E}_i$ function from Eq. (3) (blue line) with a numerical calculation for the $(\mathbf{n}\nabla)G$ source term in Eq. (1) (dashed red line). Point source located on the z axis at the point $z = -5\lambda/\pi$, $\mathbf{n} = (0,0,1)$. A blurry virtual image of this source is shown in the insert.

The functions $\mathbf{M}$, $\mathbf{N}$, and $\mathbf{L}$ are given by the formulas [9]

$$\mathbf{M}_\ell = z_\ell(\rho)[\pi_\ell(\theta)\cos\varphi\mathbf{e}_\theta - \tau_\ell(\theta)\sin\varphi\mathbf{e}_\varphi], \quad (7)$$

$$\mathbf{N}_\ell = \ell(\ell+1)\frac{z_\ell(\rho)}{\rho}P_\ell^{(1)}(\cos\theta)\cos\varphi\mathbf{e}_r + \frac{1}{\rho}\frac{d}{d\rho}[\rho z_\ell(\rho)][\tau_\ell(\theta)\cos\varphi\mathbf{e}_\theta - \pi_\ell(\theta)\sin\varphi\mathbf{e}_\vartheta], \quad (8)$$

$$\mathbf{L}_\ell = \frac{dz_\ell(\rho)}{d\rho}P_\ell^{(1)}(\cos\theta)\cos\varphi\mathbf{e}_r + \frac{z_\ell(\rho)}{\rho}[\tau_\ell(\theta)\cos\varphi\mathbf{e}_\theta - \pi_\ell(\theta)\sin\varphi\mathbf{e}_\varphi]. \quad (9)$$

Here, $z_\ell(\rho) = j_\ell(k_2 r)$ for $r < R$, $z_\ell(\rho) = h_\ell(k_1 r)$for $r > R$, $k_{1,2} = kn_{1,2}$, j_ℓ is the spherical Bessel function, h_ℓ is the spherical Hankel function of the first kind, $\pi_\ell = P_\ell^{(1)}(\cos\theta)/\sin\theta$, $\tau_\ell = dP_\ell^{(1)}(\cos\theta)/d\theta$. The quantities of magnetic fields are determined from (5) and (6) by Maxwell's equations. The scattering coefficients a, b, c, d, f, and t are found from six boundary conditions on the surface of the sphere:

$$E_\theta^{(1)} = E_\theta^{(2)}, \quad E_\varphi^{(1)} = E_\varphi^{(2)}, \quad H_\theta^{(1)} = H_\theta^{(2)}, \quad H_\varphi^{(1)} = H_\varphi^{(2)}, \quad \frac{n_1^2}{\mu_1}E_r^{(1)} = \frac{n_2^2}{\mu_2}E_r^{(2)}, \quad Q_\varphi^{(1)} = Q_\varphi^{(2)}. \quad (10)$$

Here, the first four equations meet the usual conditions of continuity of tangential components of electric and magnetic fields on the surface of sphere, the fifth describes the continuity of the normal induction vector εE_r (it is more convenient for us to use the

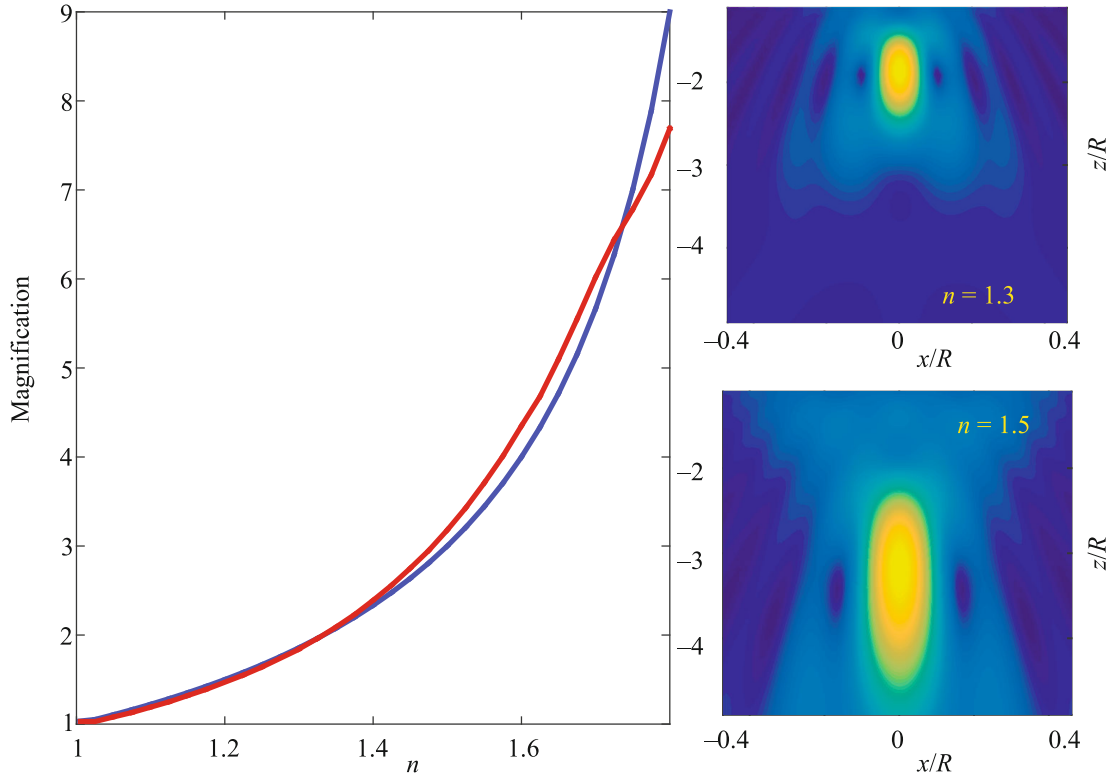

Fig. 2. (Color online) Comparison of the results of geometric (blue line) and wave (red line) optics for parameters $q = q_1 = p^{-1} = 100$. In integral (1), the domain Γ represented a square with side $2R$ and center along the z axis, at the point $z = 1.05R$. As the refractive index increases, the size of the localization region of the virtual image also increases. Blurred virtual images of a point source visible with spheres with refractive indices $n = 1.3$ and $n = 1.5$ are shown on the right side of the figure.

refractive index $n = \sqrt{\varepsilon\mu}$ instead of the dielectric permeability ε). Finally, the sixth equation describes the continuity of the longitudinal field (here, **Q** is the solenoidal part of the **E** field). The presence of longitudinal modes proportional to **L** in expansions (5) and (6) leads to the fact that all six Eq. (10) are linearly independent. This is the difference from the standard procedure in Mie theory [5, 9], where longitudinal modes play no role. However, it is precisely these modes that are important for constructing virtual images. Omitting the cumbersome calculations of the scattering coefficients from the solution of Eq. (10), we give the final formulas

$$c_\ell = iq_1 p(-1)^{\ell+1}\frac{2\ell+1}{\ell(\ell+1)}h_\ell'(q_1) \times \frac{\mu\left(j_\ell(q)[qh_\ell(q)]' - h_\ell(q)[qj_\ell(q)]'\right)}{\mu j_\ell(nq)[qh_\ell(q)]' - h_\ell(q)[nqj_\ell(nq)]'}, \quad (11)$$

$$b_\ell = iq_1 p(-1)^{\ell+1}\frac{2\ell+1}{\ell(\ell+1)}h_\ell'(q_1) \times \frac{j_\ell(q)[nqj_\ell(nq)]' - \mu j_\ell(nq)[qj_\ell(q)]'}{\mu j_\ell(nq)[qh_\ell(q)]' - h_\ell(q)[nqj_\ell(nq)]'}, \quad (12)$$

$$d_\ell = iq_1 p(-1)^{\ell}\frac{2\ell+1}{\ell(l+1)}\left[\left[\frac{h_\ell(q_1)}{q_1}\right]'(\ell+1) - h_{\ell+1}'(q_1)\right] \times \frac{\mu n\left(j_\ell(q)[qh_\ell(q)]' - h_\ell(q)[qj_\ell(q)]'\right)}{n^2 j_\ell(nq)[qh_\ell(q)]' - \mu h_\ell(q)[nqj_\ell(nq)]'}, \quad (13)$$

$$a_\ell = iq_1 p(-1)^{\ell}\frac{2\ell+1}{\ell(l+1)}\left[\left[\frac{h_\ell(q_1)}{q_1}\right]'(\ell+1) - h_{\ell+1}'(q_1)\right] \times \frac{\mu j_\ell(q)[nqj_\ell(nq)]' - n^2 j_\ell(nq)[qj_\ell(q)]'}{n^2 j_\ell(nq)[qh_\ell(q)]' - \mu h_\ell(q)[nqj_\ell(nq)]'}, \quad (14)$$

$$t_\ell = iq_1 p(-1)^{\ell}(2l+1) \times \left[\frac{h_\ell(q_1)}{q_1}\right]'\frac{\mu n(j_\ell(q)h_\ell'(q) - h_\ell(q)j_\ell'(q))}{\mu j_\ell(nq)h_\ell'(q) - n^3 h_\ell(q)j_\ell'(nq)}, \quad (15)$$

$$f_\ell = iq_1 p(-1)^{\ell}(2l+1) \times \left[\frac{h_\ell(q_1)}{q_1}\right]'\frac{n^3 j_\ell(q)j_\ell'(nq) - \mu j_\ell(nq)j_\ell'(q)}{\mu j_\ell(nq)h_\ell'(q) - n^3 h_\ell(q)j_\ell'(nq)}. \quad (16)$$

Here, $q = kR$, $q_1 = kr_0$, $n = n_2/n_1$, $\mu = \mu_2/\mu_1$, prime means differentiation by argument. In the limit, when the point source moves away to infinity, functions t

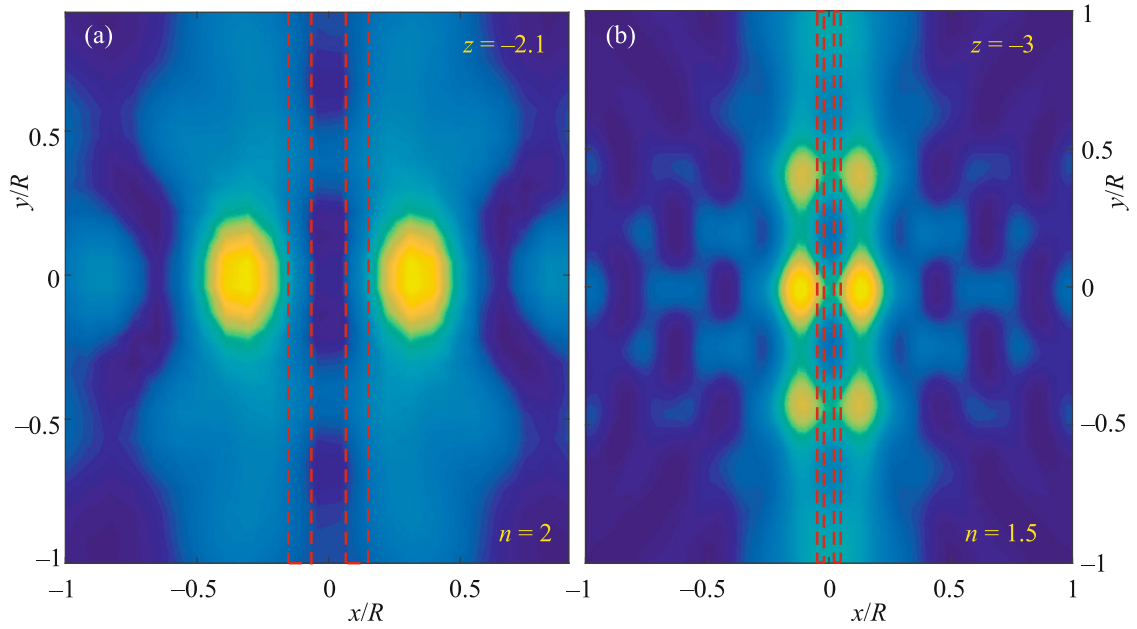

Fig. 3. (Color online) Virtual image of two slits with a width of λ/6 and a distance between them λ/4 (a) and λ/6 (b). The position of the slits is shown with dashed lines. Parameter values: (a) $n = 2$, $q = 12$ and (b) $n = 1.5$, $q = 38$. The virtual images are located at the distances: (a) $z = -2.1R$ and (b) $z = -3R$. The slit fields add up in an incoherent way. The slit radiation (a) is polarized along the x axis. In the slots (b) $\mathbf{E}^0(-1, 0, 0.5)$ for the right and $\mathbf{E}^0(1, 0, 0.5)$ for the left slots, respectively. When constructing, only the x polarization of the field $\mathbf{E}_i$ was considered.

and f tend to zero, and the coefficients a, b, c, d tend to their expressions in the Mie theory; in this case, one should set $p = \exp(-iq_1)$. The factor $-i$ in these limiting formulas arises from the derivative of the delta function of the selected point source (4). The position of the virtual image was determined by Eq. (1), as the point of the local maximum of the field $\mathbf{E}_i$. The dependence of the magnification factor of the virtual image M on the value of the relative refractive index is shown in Fig. 2. The graph also shows the magnification factor at the geometric optics limit. Despite the fact that in the given example the formal requirements of geometric optics are fulfilled: $q \gg 1$, $q_1 \gg 1$, the difference between the two dependences, as expected, increases as the refractive index approaches two.

Now let us turn to the question of overcoming the diffraction limit for the virtual image. The possibility of such a phenomenon in the wave theories has not yet been studied. From the experiments [3, 4, 10, 11] it follows that the diffraction limit is overcome at certain parameters of the sphere. Since the data on the resolution of the periodic system of the dark and light stripes are most often encountered in experiments (usually nanosized strips recorded on *Blu-ray disk*), to begin with we will consider the resolution field from the slot according to Eq. (2). For building solutions, we use auxiliary solutions ζ_i^j for fields of the form $\dfrac{\partial G(\mathbf{r}, \mathbf{r}_0)}{k\partial x^j}\mathbf{e}_i$, where $\mathbf{r}_0$ describes arbitrary position of the source in space. Solution (2) in this case, due to linearity, has the form:

$$X = \frac{(-2)}{4\pi}\iint_{\Sigma} E_i^0 n^j \zeta_i^j k^2 dS, \qquad (17)$$

where X is one of the components of the scattered field (in program in MATLAB first, the coefficients (11)–(16) are calculated, and then the fields themselves are constructed).

Calculations using the above formulas show that the diffraction limit is indeed overcome in a certain range of sphere parameters. Figure 3 shows two examples where in the virtual image, two adjacent bright stripes are located at distances λ/4 and λ/6 from each other. In the given examples, the slits are considered incoherent with respect to each other, but the sources inside each of the slits are coherent. The above theory does not consider the possible change in the field $\mathbf{E}^0$ inside the slot itself, as well as the self-consistent calculation of the field $\mathbf{E}^0$ due to the effect of the sphere backscattering. Effects of this kind play an important role in the "particle on a substrate" problem [12, 13]. However, even in the considered approximation, the wave theory answers affirmatively to the question of the possibility of overcoming the diffraction limit in the virtual image.

A theoretical resolution limit based on the above formulas is possible, but it requires large numerical calculations associated with finding the maximum

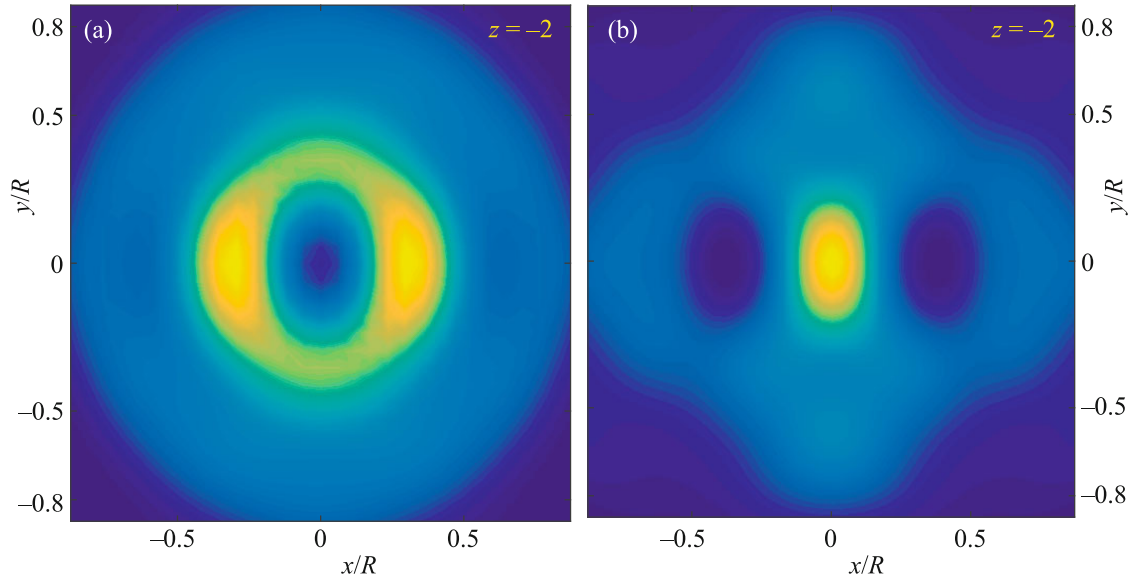

Fig. 4. (Color online) (a) Virtual image of a source located on the z axis ($z = -R$) as a dark dot on a light background. (b) A virtual image of two sources located symmetrically along the x axis at the distance λ from each other, $z = -R$. Problem parameters: $q = 18$, $n = 2$, the position of the virtual image in the plane $z = -2R$.

resolution in the five-dimensional space of parameters: the size of the sphere, the refractive index, and $\{x_0, y_0, z_0\}$ coordinates describing the position of the source (in the general case, one should also take into account polarization and slit shape). The experimentally confirmed resolution of the virtual image in the visible region is $\lambda/8$ [3, 4]. This theory also explains the experimentally observed effect when, in a certain range of parameters, the light slits in the virtual image look dark, and the dark areas between the slits look light. In essence, this is the reincarnation of a well-known phenomenon in the theory of diffraction, when a bright spot is observed in the center of the image of an opaque disk, corresponding to half of the action of the first open Fresnel zone [5]. The corresponding pictures of the virtual image are shown in Fig. 4.

CONCLUSIONS

The proposed method of forming an optical image by constructing a virtual converging wave makes it possible to find the parameters of a virtual image in the region where geometric optics is inapplicable. The method allows one to define the resolution image parameters beyond the diffraction limit.

FUNDING

This work was supported by the Ministry of Science and Higher Education of the Russian Federation (project no. 14.W03.31.0008), in part by the Russian Science Foundation (project no. 20-12-00389), and in part the Russian Foundation for Basic Research (project no. 20-02-00715).

REFERENCES

1. B. S. Luk'yanchuk, R. Paniagua-Dominguez, I. Minin, O. Minin, and Z. B. Wang, Opt. Mater. Express **7**, 1820 (2017).
2. A. I. Kuznetsov, A. E. Miroshnichenko, M. L. Brongersma, Y. S. Kivshar, and B. Luk'yanchuk, Science (Washington, DC, U. S.) **354**, aag2472 (2016).
3. Z. B. Wang, W. Guo, L. Li, B. Luk'yanchuk, A. Khan, Z. Liu, Z. Chen, and M. H. Hong, Nat. Commun. **2**, 218 (2011).
4. *Label-Free Super-Resolution Microscopy,* Ed. by V. Astratov (Springer, Cham, Switzerland, 2019), p. 371.
5. M. Born and E. Wolf, *Principles of Optics: Electromagnetic Theory of Propagation, Interference, and Diffraction of Light* (Elsevier, Amsterdam, Netherlands, 2013).
6. S. Solimeno, B. Crosignani, and P. di Porto, *Guiding, Diffraction, and Confinement of Optical Radiation* (Academic, New York, 1986).
7. H. Chew, P. J. McNulty, and M. Kerker, Phys. Rev. A **13**, 396 (1976).
8. H. Chew, M. Kerker, and D. D. Cooke, Phys. Rev. A **16**, 320 (1977).
9. C. F. Bohren and D. R. Huffman, *Absorption and Scattering of Light by Small Particles* (Wiley, Hoboken, New Jersey, 1998).
10. L. A. Krivitsky, J. J. Wang, Z. B. Wang, and B. Luk'yanchuk, Sci. Rep. **3**, 3501 (2013).
11. K. W. Allen, N. Farahi, Y. Li, N. I. Limberopoulos, D. E. Walker, Jr., A. M. Urbas, V. Liberman, and V. N. Astratov, Ann. Phys. **527**, 513 (2015).
12. B. S. Luk'yanchuk, Y. W. Zheng, and Y. F. Lu, Proc. SPIE **4065**, 576 (2000).
13. D. Bedeaux and J. Vlieger, *Optical Properties of Surfaces* (Imperial College Press, London, 2004).